ACCOUNTS
of chemical research

Bioinspired Super-antiwetting Interfaces with Special Liquid–Solid Adhesion

MINGJIE LIU,[‡] YONGMEI ZHENG,[§] JIN ZHAI,[§] AND LEI JIANG*,[†,§]

[†]*Beijing National Laboratory for Molecular Sciences (BNLMS), Center for Molecular Sciences, Institute of Chemistry, Chinese Academy of Sciences, Beijing 100190, P. R. China,* [‡]*National Centre for NanoScience and Technology, Beijing 100190, P. R. China, and* [§]*School of Chemistry and Environment, Beijing University of Aeronautics and Astronautics, Beijing 100191, P. R. China*

RECEIVED ON JULY 16, 2009

CONSPECTUS

Super-antiwetting interfaces, such as superhydrophobic and superamphiphobic surfaces in air and superoleophobic interfaces in water, with special liquid–solid adhesion have recently attracted worldwide attention. Through tuning surface microstructures and compositions to achieve certain solid/liquid contact modes, we can effectively control the liquid–solid adhesion in a super-antiwetting state. In this Account, we review our recent progress in the design and fabrication of these bioinspired super-antiwetting interfaces with special liquid–solid adhesion.

Low-adhesion superhydrophobic surfaces are biologically inspired, typically by the lotus leaf. Wettability investigated at micro- and nanoscale reveals that the low adhesion of the lotus surface originates from the composite contact mode, a microdroplet bridging several contacts, within the hierarchical structures. Recently high-adhesion superhydrophobic surfaces have also attracted research attention. These surfaces are inspired by the surfaces of gecko feet and rose petals. Accordingly, we propose two biomimetic approaches for the fabrication of high-adhesion superhydrophobic surfaces. First, to mimic a sticky gecko's foot, we designed structures with nanoscale pores that could trap air isolated from the atmosphere. In this case, the negative pressure induced by the volume change of sealed air as the droplet is pulled away from surface can produce a normal adhesive force. Second, we constructed microstructures with size and topography similar to that of a rose petal. The resulting materials hold air gaps in their nanoscale folds, controlling the superhydrophobicity in a Wenzel state on the microscale.

Furthermore, we can tune the liquid–solid adhesion on the same superhydrophobic surface by dynamically controlling the orientations of microstructures without altering the surface composition. The superhydrophobic wings of the butterfly (*Morpho aega*) show directional adhesion: a droplet easily rolls off the surface of wings along one direction but is pinned tightly against rolling in the opposite direction. Through coordinating the stimuli-responsive materials and appropriate surface-geometry structures, we developed materials with reversible transitions between a low-adhesive rolling state and a high-adhesive pinning state for water droplets on the superhydrophobic surfaces, which were controlled by temperature and magnetic and electric fields.

In addition to the experiments done in air, we also demonstrated bioinspired superoleophobic water/solid interfaces with special adhesion to underwater oil droplets and platelets. In these experiments, the high content of water trapped in the micro- and nanostructures played a key role in reducing the adhesion of the oil droplets and platelets. These findings will offer innovative insights into the design of novel antibioadhesion materials.

Published on the Web 12/02/2009 www.pubs.acs.org/acr
10.1021/ar900205g

Introduction

The design and creation of novel super-antiwetting interfaces,[1] such as superhydrophobic[2] and superamphiphobic[3,4] surfaces in air and superoleophobic interfaces in water,[5] has been inspired by biological surfaces with special wettability. These novel super-antiwetting interfaces have attracted considerable attention due to their great advantages in both fundamental research and practical applications.[6,7] In particular, the super-antiwetting interfaces with special liquid−solid adhesion have recently aroused extensive interest. For instance, liquid−solid adhesion is greatly decreased by micro- and nanostructures on the surface of the superhydrophobic lotus leaf, which is necessary for its self-cleaning property.[8] Water droplets do not stably remain on the surface but easily roll off and spontaneously remove dust particles on the leaf. In a similar manner to the lotus effect in the atmosphere, fishes can resist pollution by oil in water due to the roughness of their scales forming a low adhesion and superoleophobic water/solid interface, which would suggest a new strategy to design novel antibioadhesion materials underwater.[5]

On the other hand, superhydrophobic surfaces with high liquid−solid adhesion become a new focus for their potential applications in liquid transportation, biochemical separation, *in situ* detection, and localized chemical reaction.[9−12] A water droplet on these surfaces shows a static contact angle (CA) larger than 150°, but the droplet is pinned on the surfaces at any tilted angles. The achievement of such a high adhesion at the liquid−solid interface is inspired by the gecko's attachment system and rose petals.[10,13] For example, by mimicking the special structures on the gecko's feet, we reported an aligned polystyrene (PS) nanotube film with superhydrophobicity and high adhesion to water, which could be used as a "mechanical hand" for reversible no-loss transport of microdroplets.[14]

Generally, the liquid−solid adhesion is mainly governed by the surface geometrical structure and surface composition. Therefore, through dynamically tuning the two factors, the liquid−solid adhesion could be effectively controlled.[15−20] Moreover, through modifying the stimuli-responsive materials on solid substrates, superhydrophobic surfaces with switchable liquid−solid adhesion under external stimuli could be achieved.[21,22] These superhydrophobic surfaces with controllable liquid−solid adhesion can be used for the construction of future generation smart devices.

In this Account, we will review our recent progress on bioinspired super-antiwetting interfaces with special liquid−solid adhesion. First, we will present some basic theories on liquid−solid adhesion. In the following two sections, we will review the low- and high-adhesion superhydrophobic surfaces with particular focus on how to design high-adhesion superhydrophobic surfaces. Then, we will demonstrate the origins of directional adhesion, examining how the arrangement and orientation of micro- and nanostructures are used to control adhesion. Next, we will show some stimuli-responsive switching between low and high adhesion. Finally, the wetting behavior in an oil/water/solid system is described, which could help us understand the adhesion between a platelet and a solid surface.

Basic Theories of Liquid−Solid Adhesion on Superhydrophobic Surfaces

Generally, surfaces with a static CA higher than 150° are defined as superhydrophobic surfaces.[1] It should be noted that even if the superhydrophobic surfaces exhibit comparable apparent CAs, their adhesion to liquid may be quite different.[23,24] Whether a droplet could be pinned on a superhydrophobic surface is ascribed to the distinct contact modes[23,25] (the Wenzel state or the Cassie state) and the triple-phase liquid/air/solid contact line (TCL).[26,27] In the Wenzel state,[28] a water droplet fully penetrates into the valleys of a textured surface (in wet contact mode), and the TCL is continuous and stable. Thus the surface generates relatively high adhesion, accordingly, to pin the droplet. In contrast, in the Cassie state,[29] the water droplet is suspended by the vapor pockets trapped on surface (in composite contact mode), and TCL is discontinuous. Thus the adhesion of the surface is relatively decreased, and the droplet easily rolls off the surface. However, in most cases, a water droplet may partially wet a superhydrophobic textured surface due to air partially trapped in the valleys, which is an intermediate state between Wenzel and Cassie states. Such an intermediate state of solid/liquid contact is referred to as a metastable state.[23,30] This indicates that a transition between these two superhydrophobic states could be achieved on the same microstructured surface when external stimuli (like a pressing force) exists.[23] In addition, the superhydrophobic states may be tuned between the Wenzel state with high adhesion and the Cassie state with low adhesion through the design of robust microstructures with variable geometric parameters to control certain solid/liquid contact modes.[31−33]

Normally, the liquid−solid adhesion is assessed by the contact angle hysteresis (CAH), which is defined as the difference between advancing and receding CAs. The CAH can be influenced by the surface structure, chemical heterogeneity, TCL, etc.[34−38] However, the measurement of CAH only indicates

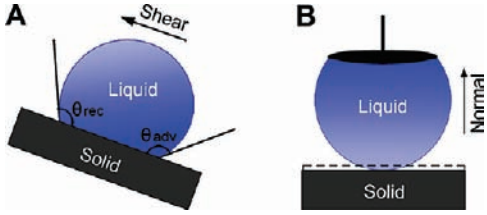

FIGURE 1. Schematic illustration of two models for adhesion characterization: (A) CAH measurement, indicating an adhesion along the shear direction; (B) NAF measurement, indicating an adhesion along the normal direction.

effects of adhesion along the shear direction (Figure 1A).[39] To thoroughly understand the adhesion behavior between liquid and solid, the normal adhesive force (NAF) should be also taken into account. For example, if a water droplet sticks to the high-adhesion superhydrophobic surface, it will not roll away even if the surface is tilted a high angle or turned upside down. In this case, the CAH is not suitable to quantitatively study the adhesive force.[40] To solve the problem, a high-sensitivity balance system is used to quantitate the NAF between the water droplet and the superhydrophobic surface.[10] As shown in Figure 1B, a liquid droplet is suspended on the balance system, and the surface is controlled to contact and leave the droplet. The force required to take the droplet away from the surface is thought to be the NAF between liquid and solid, which is related to the preload, the volume of droplet, etc. The CAH and NAF are two independent and complementary methods to characterize adhesion properties. In the following sections, both types of adhesive force are taken into account according to the practical case.

Low-Adhesion Superhydrophobic Surfaces

Many biological surfaces, such as plant leaves[2] and water strider's legs,[41] possess superhydrophobic and low-adhesion properties. The self-cleaning lotus leaf is among the most famous examples. Water droplets on its surface are almost spherical and can roll off easily at small inclinations, which is known as the "lotus effect". In this section, some typical studies from different views on lotus leaf will be introduced.

The microscopic details of wetting behavior on the lotus-leaf surface were studied by environmental scanning electron microscopy (ESEM)[42] and an atomic force microscopy (AFM) system,[43] which can help us well understand the origin of low adhesion. According to the ESEM observations, it can be seen that the leaf surface is composed of numbers of papillae and each papilla is covered with countless nanohairs (Figure 2A,B). A microdroplet is suspended on the tops of the papillae and bridges them, displaying a composite contact mode from the side-view of the droplet (Figure 2C). To further investigate the interface between the papillae and water droplet, a droplet-inside-view based on the AFM system was introduced (Figure 2D). The topographic (Figure 2E) and deflection images (Figure 2F) display the real state of the macroscopic water/air/solid interface for the lotus leaf underneath the water droplet. It can be seen that air is trapped in the micro- and nanoscale structures to form air layers. The ESEM and AFM observations fully demonstrated how the composite contact mode arises from the presence of air trapped at the micro- and nanoscales as the Cassie state describes. Therefore, the adhesion between liquid and solid greatly decreased due to such a composite contact mode.

Interestingly, when we shifted the focus from the upper surface to the leaf margin, we found that water on the upper lotus leaf can be easily shed from the surface through the margin, while the water underneath the lotus leaf hardly overflows, even pressing the lotus leaf to a certain depth (Figure

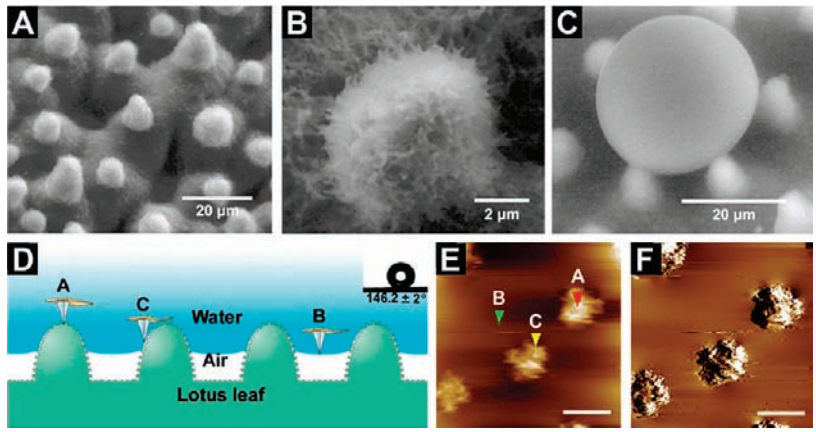

FIGURE 2. Topography of the lotus leaf surface and investigation of wetting behavior at the microscale: (A) valleys surrounded with multipapillae; (B) papilla with nanohairs; (C) a microdroplet in the valley is suspended by multipapillae; (D) schematic representation of imaging by AFM in the Cassie state; (E) topographic image taken in contact mode (scale bar = 7.5 μm); (F) corresponding deflection image of panel E (scale bar = 10 μm).

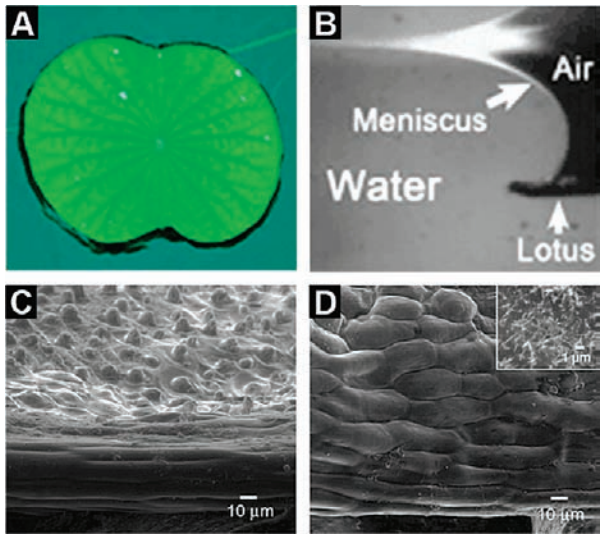

FIGURE 3. (A) A photo of a lotus leaf on water, (B) an optical microscopic image of a lotus surface as pressed into water, (C) an ESEM image of a lotus leaf including the margin and papillae, and (D) an ESEM image of the leaf margin. The inset is the magnified image of a nanoscale wax crystal.

3A,B). Our recent research highlighted the role of the leaf margin in restricting fluid and resolved the mechanism behind the phenomenon.[44] It is mainly attributed to the anisotropic topography composed of microfolds at the margin, which are quite different from papillae with micro- and nanohierarchical structures on the upper surface (Figure 3C). The microfolds around the leaf margin form a ring-band (Figure 3D), which introduces a strong energy barrier against water that tends to return to the surface. As a result, the water underneath the lotus surface hardly overflows onto the upper surface. This finding can help us fully understand the lotus effect and inspire us to design a novel microdevice that can run on water or a self-cleaning surface with smart margin.

High-Adhesion Superhydrophobic Surfaces

In contrast to low-adhesion superhydrophobic surfaces, there are some surfaces on which a water droplet shows a static CA larger than 150° but it is pinned on the surfaces at any tilted angle. The achievement of such high adhesion is inspired by the gecko's attachment system and rose petals. Accordingly, two biomimetic approaches are proposed to fabricate high-adhesion superhydrophobic surfaces, which will be introduced in this section.

One approach is inspired by the gecko, which can firmly attach to various surfaces. This remarkable adhesive ability of gecko arises from millions of nanoscale foot hairs on its feet.[45] Based on the recognition of the gecko's attachment system, we fabricated a superhydrophobic PS nanotube film by mimicking the gecko's feet.[10] The film can hold a water droplet even if it is turned upside down, showing a high adhesion to water. The NAF assessed by a high-sensitivity microelectromechanical balance system is about 59.8 μN. Detailed scanning electron microscopy (SEM) images show that the as-prepared PS film is composed of densely packed aligned nanotubes (Figure 4A). It is assumed that the special nanotubular structures can induce two kinds of trapped air; there are air pockets in the open state (continuous with the atmosphere), as well as sealed air pockets trapped in the PS nanotubes. For a static water droplet on the surface, the role of the trapped air is to induce a high CA; the adhesive force between the water and surface arises from van der Waals' interactions. Once the water droplet is drawn, the NAF may be produced

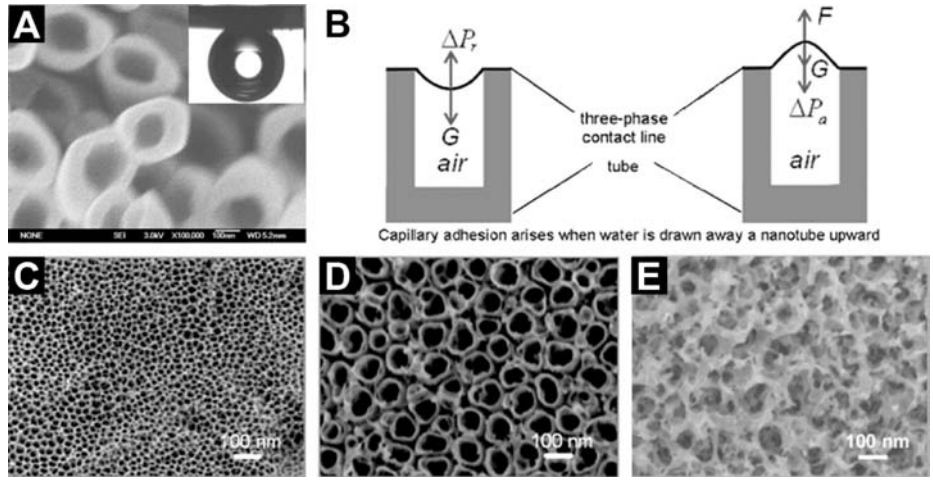

FIGURE 4. SEM images of designed superhydrophobic surfaces with different adhesion and schematic illustration: (A) the aligned PS nanotube layer; in the inset, the shape of water on the PS surface when it is turned upside down; (B) schematic illustration of NAF caused by negative pressure when a water droplet is drawn away; (C–E) top view of a superhydrophobic TiO_2 (C) nanopore array, (D) nanotube array, and (E) nanovesuvianite structures.

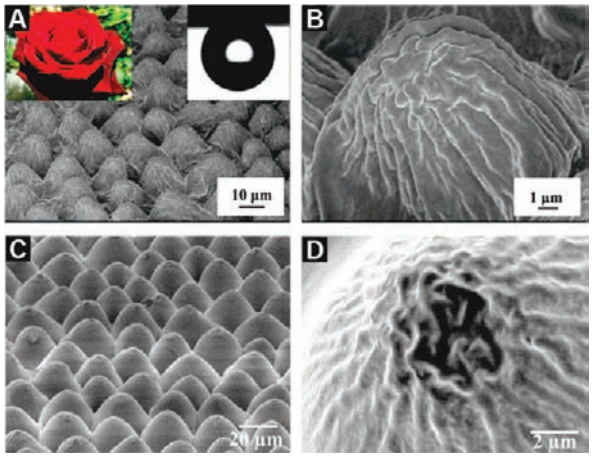

FIGURE 5. The structures of rose petals and obtained replica: (A, B) SEM images of rose petal's surface at low and high magnifications; in the inset, the shape of water on the petal's surface when it is turned upside down; (C, D) SEM images of the obtained PDMS replica at low and high magnifications.

by the negative pressure induced by the volume change of the sealed air in the nanotubes (Figure 4B). To prove the mechanism of high adhesion, we designed three types of superhydrophobic nanostructure models consisting of a nanopore array (Figure 4C), a nanotube array (Figure 4D), and nanovesuvianite structures (Figure 4E).[46] When a water droplet contacts the solid surface, sealed air pockets could be formed in the nanopore array and nanotube array surfaces, while only open air pockets could be formed in the nanovesuvianite surface. As a result, the NAF plays a dominant role in enhancing adhesion behavior on the nanopore array and nanotube array surfaces, while the nanovesuvianite surface showed extremely low adhesion to water.

The other approach is inspired by rose petals. For example, in nature, when tiny raindrops land on rose petals, they are almost spherical but resist rolling off the flower (inset of Figure 5A).[13] The spherical water droplets that glitter in the sun are expected to attract insects for pollination. To illustrate the origin of this high adhesion, we studied the microstructures of the rose petal. Figure 5A exhibits a periodic array of micropapillae compactly arranged on the rose petal. There exist nanoscaled cuticular folds on the top of the micropapillae (Figure 5B). A water droplet on the petal's surface is expected to penetrate into the microscale grooves, but air gaps are present in the nanoscale folds, thus forming a partial Wenzel state. It can be readily understood that water sealed in micropapillae would cling to the petal's surface, resulting in a strong adhesion between solid surface and liquid. The understanding of the rose petal inspires us to fabricate biomimic polymer films that possess both superhydrophobicity and the high-adhesion property. For example, we used PS and polydimethylsiloxane (PDMS) to directly duplicate the microstructures of rose petals (Figure 5C,D).[47] The resulting surfaces have the same microstructures and high-adhesion property.

High-adhesion superhydrophobic surfaces provide effective solutions to transport small volumes of liquids. One example is the application of the superhydrophobic PS nanotube film as a "mechanical hand" in no-loss transport of a superparamagnetic microdroplet (*M*-droplet).[14] When the upper magnet is applied, the *M*-droplet flies upward and is stuck to the PS nanotube film due to the strong adhesive effect. When the magnet force is reversed, the *M*-droplet falls back to the ordinary superhydrophobic surface. The key point of this application is no loss of the *M*-droplet during the reversible transport.

In this section, two biomimetic approaches for fabricating high-adhesion superhydrophobic surfaces are described: One is the design of structures with nanoscale pores that could possibly trap air isolated from the atmosphere. This trapped air increases the adhesion because of a negative pressure induced by an increase in volume of an air pocket as the droplet is pulled away from the surface. The other is the construction of microstructures with appropriate size and topography to control the superhydrophobic state in the Wenzel state.

Directional Adhesion Superhydrophobic Surfaces

Besides isotropic adhesion on natural superhydrophobic surfaces such as lotus leaves and petals, anisotropic adhesion can also be seen in nature, for example, rice leaves, which have offered a robust model to regulate fluid.[2] It is generally recognized that anisotropic liquid−solid adhesion is ascribed to the arrangement and orientation of micro- and nanostructures.[48,49] Directional adhesion on the superhydrophobic wings of a butterfly (*Morpho aega*) is an example (Figure 6A).[50] A water droplet can easily roll off the surface of the wings along the radial outward (RO) direction of the central axis of the body, but is tightly pinned in the opposite direction (Figure 6B,C). Interestingly, these two distinct states can be tuned by controlling the posture of the wings (downward or upward) and the direction of airflow across the surface (along or against the RO direction). It is demonstrated that this unique ability is ascribed to the direction-dependent arrangement of flexible nanotips on the top of ridging nanostrips and microscales overlapped on the wings at the one-dimensional level (Figure 6D,E).

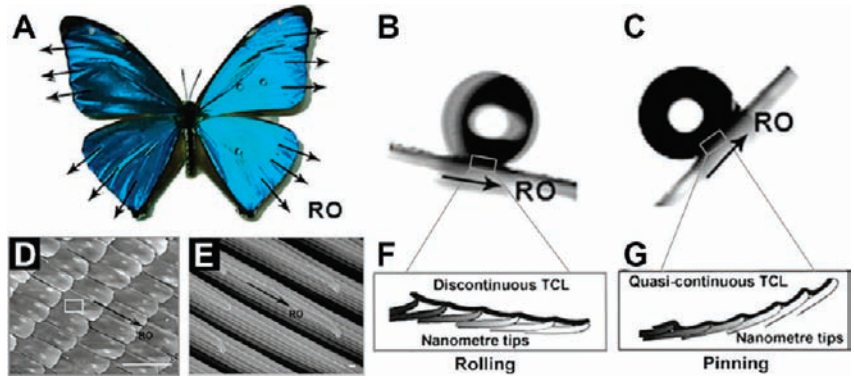

FIGURE 6. Directional adhesion on superhydrophobic butterfly wings and SEM images of the wings: (A) an iridescent blue butterfly, *M. aega*; the black arrows denote the RO direction away from the body's center axis; (B) the droplet easily rolls along the RO direction when the wing is tilted toward downward by 9°; (C) the droplet pinned on the wing that is tilted upward; (D, E) SEM images of the wings (scale bars = (D) 100 μm and (E) 100 nm). (F, G) two models proposed for the potential mechanism of distinct adhesion—(F) rolling state and (G) pinning state.

Two distinct contact modes of a water droplet coexist on the orientation-tunable microstructured surface and thus produce contrasting adhesion. When the wing is tilted down, the oriented nanotips on the nanostrips and microscales separate from each other. The water droplet on the wing not only presents a "composite" contact with the top of the nanostripes and a "dry" contact with the air trapped in the nanogrooves but also forms a discontinuous TCL, which makes it easily roll off the surface (Figure 6F). When the wing is tilted upward, the flexible nanotip and microscales take a close arrangement. The water droplet is in the "wet" contact with the nanostrips and forms a quasi-continuous TCL, which pins it on the surface (Figure 6G).

To understand the directional liquid—solid adhesion resulting from the oriented micro- and nanostructures on the butterfly wings, we fabricated a microscale ratchet structure into aluminum alloy surfaces to mimic the step-overlapping structure of the butterfly's wing.[51] This ratchet structure enables the *M*-droplet to generate anisotropic behavior through the external alternative magnetic field. As shown in Figure 7, there is no difference when the *M*-droplet slides on the flat structured surface along both directions (Figure 7A), whereas *M*-droplets deform distinctly on the ratchet structured superhydrophobic surface. An *M*-droplet moving along direction 1 has a vertical oscillation like a "water spring" during the process of advancing after it overcomes the adhesion to move (Figure 7B), whereas an *M*-droplet moving along direction 2 seems to be rather wormed (Figure 7C). Along direction 1, the CAH corresponding to the surface adhesion is ~26.3°; whereas along direction 2, CAH is ~62.2°, which is far higher adhesion than that in direction 1. The decreasing adhesion is attributed to a relatively lower solid—liquid contact extent along direction 1, while this case is opposite along direction 2. This study indicates that an asymmetric ratchet introduces different behaviors of an *M*-droplet on a superhydrophobic surface, which implies a distinct directional adhesion by means of the ratchet structure.

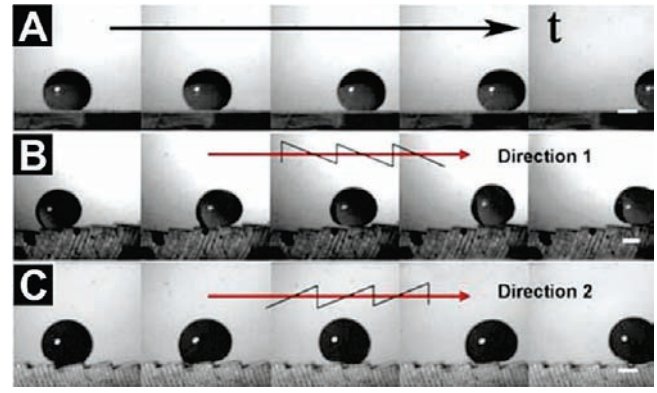

FIGURE 7. The time-sequence optical images of an *M*-droplet moving on the flat surface (A) and ratchet-structured superhydrophobic surfaces along directions 1 (B) and 2 (C). Scale bar = 1 mm.

Stimuli-Responsive Adhesion on Superhydrophobic Surfaces

As discussed above, a liquid droplet on superhydrophobic surfaces in the Wenzel or Cassie state will show different adhesion. It is reported that there are energy barriers to prevent the transition between these two states.[23,52] Smart materials that can alter surface chemical properties via external stimuli provide an effective approach to conquer the energy barrier of the wetting state transition. Therefore, reversible switching of solid—liquid adhesion on superhydrophobic surfaces can be achieved with the precise coordination of surface chemistry response and surface roughness.

To verify this idea, we modified a side chain liquid crystal polymer, PDMS-4OCB, a thermal responsive polymer, on a silicon surface.[22] On the flat PDMS-4OCB film, the water CA changes from 92.4° to 89.3° when the temperature increases

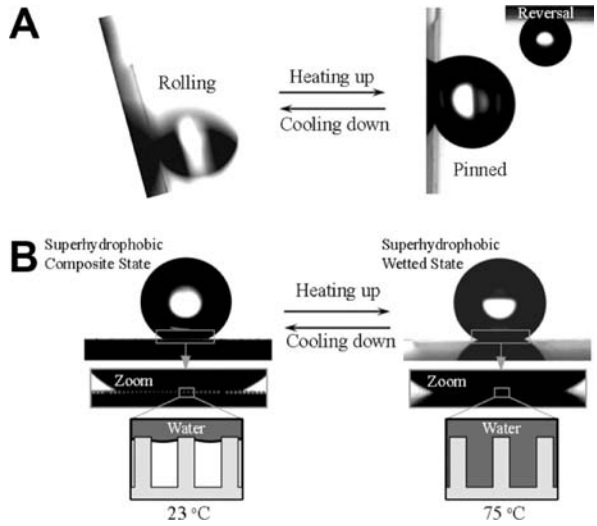

FIGURE 8. (A) Reversible switching of a water droplet's mobility from rolling to pinning corresponding to the temperature switch from 23 (left) to 75 °C (right, the inset shows that the droplet sticks on the surface even when the substrate is turned upside down). (B) At 23 °C, the water droplet is in the composite state (Cassie state); at 75 °C, it is in the wetted state (Wenzel state).

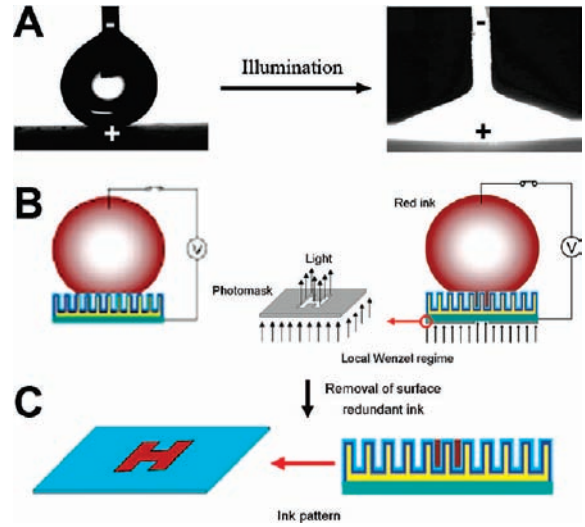

FIGURE 9. Photoelectric cooperative wetting on the ACNA surface: (A) before and after the light is turned on; (B) surface wettability locally transits from Cassie to Wenzel states with the patterned light "H" illumination to the ACNA; (C) an ink-patterned "H" is left with the removal of redundant ink.

from 23 to 75 °C (just above the phase transition point), which corresponds to the discontinuous interfacial action change for the liquid crystal to isotropic phase transition. On an optimized rough silicon wafer, the static water CAs are all at superhydrophobic level, but the CAH is dramatically different upon tuning the temperature. The mobility of a water droplet on this superhydrophobic surface can be thermally controlled from rolling (CAH $\approx$ 75°) to pinning state (Figure 8A). It can be judged that a water droplet is in the Cassie state at 23 °C and the Wenzel state at 75 °C according to whether there is light gap between the liquid and the substrate from a microscopic side view (Figure 8B). This result indicates that the switching of adhesion is dependent on the wetting state transition.

Switchable adhesion can also be observed on a superhydrophobic iron surface.[21] An *M*-droplet on it could be reversibly controlled from rolling to pinning state by altering magnet field. Before the iron surface is magnetized or after demagnetization, the magnetic domains of the iron surface are unordered. Such a surface cannot lead to the magnetization of Fe_3O_4 nanoparticles in the *M*-droplet, so there is no magnetic force between them and the *M*-droplet resides in the low-adhesive Cassie state. After the iron plate is magnetized, the magnetic domains of iron are orderly arrays, and such a surface can bring on the magnetization of Fe_3O_4 nanoparticles, so the magnetic force is produced. Accordingly, the *M*-droplet resides in the high-adhesive Wenzel state.

Compared with above techniques, electrowetting is a more mature technique that can induce a transition of droplets from Cassie to Wenzel state.[53] However, traditional electrowetting always happens on a liquid−solid contact area, which cannot realize a localized controlled wetting state transition. Recently, we realized a precise controllable patterned wetting state transition on the superhydrophobic aligned composite nanorod array (ACNA) surface via a photoelectric cooperative wetting process (Figure 9A).[54] Based on this technique, a localized liquid−solid adhesion switching could be achieved on superhydrophobic surfaces. For example, when a drop of water-soluble red ink is placed onto the ACNA surface below the threshold voltage, air is trapped in the troughs between the individual nanorods. With the patterned light "H" illuminating the ACNA surface, the wettability of the patterned site transfers from Cassie to Wenzel state, and thus the red ink enters into the troughs (Figure 9B). As a result, an ink pattern "H" is adhered on the surface, while the redundant ink can be easily removed (Figure 9C).

In the Oil/Water/Solid System: Bioinspired Superoleophobic Water/Solid Interfaces with Structure-Tunable Adhesion

The wetting/antiwetting behavior of liquid droplets on the solid surface is not an apparent or simple contact between two phases but one among three phases. Biomimetic research on the self-cleaning effect of fish scales indicates that superhydrophilic surfaces in the water/air/solid system show superoleophobic properties in an oil/water/solid system by replacing the air phase with a water phase.[5]

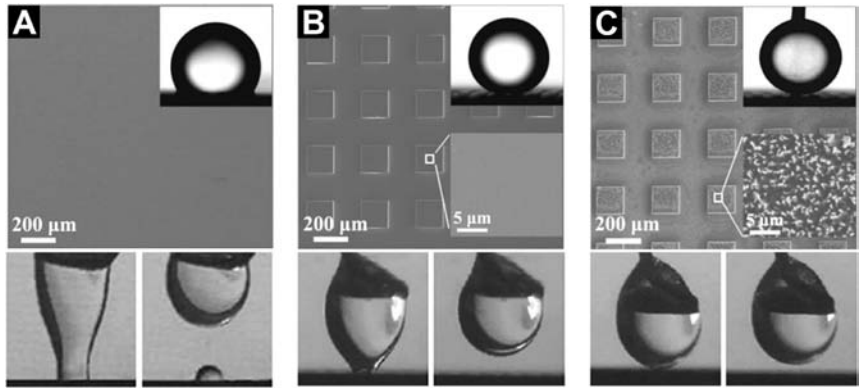

FIGURE 10. SEM images of the substrates and shapes of oil droplets taken at different stages during the NAF measurement process on different substrates: on the (A) smooth, (B) microstructured, and (C) micro/nanostructured silicon substrate.

To understand the detailed wetting behavior in the oil/water/solid system, smooth, microstructured, and micro- and nanohierarchical structured silicon surfaces were selected as our modeling ones. We observed that the smooth silicon surface is oleophobic with a CA of 134.8° (Figure 10A), while the microstructured and micro/nanostructured silicon surfaces show superoleophobicity with CAs larger than 150° (Figure. 10B,C). However, they are significantly different in adhesive behaviors. The smooth silicon surface exhibits remarkable adhesion to an oil droplet, which always draws an oil droplet with great shape distortion and then causes it to break (Figure 10A). The NAF is larger than the stretching force, 24.7 μN. For the microstructured silicon surface, the oil droplet can be only stretched to an elliptical shape (Figure 10B). The NAF measured is about 10.2 μN. However, for the micro/nanostructured silicon surface, the shape of the oil droplet remains spherical during the whole measurement, implying the the NAF is smaller than 1 μN (Figure 10C). In the oil/water/solid system, the adhesive property remains consistent with that of a water/air/solid system. When the surfaces contact with the oil droplet, water molecules can be trapped in the micro/nanostructures, which forms an oil/water/solid composite interface. These trapped water molecules will greatly decrease the adhesive force between the oil droplet and the solid surface.

Compared with superhydrophobic surfaces in the water/air/solid system, we believe that superoleophobic surfaces in the oil/water/solid system are more interesting and important for antibioadhesion applications. For example, we constructed a nanoscale topography on a thermally responsive poly(*N*-isopropylacrylamide) (PNIPAAm) surface by grafting the polymer from silicon nanowire arrays.[55] The as-prepared surface shows superoleophobic behavior and low adhesion to oil droplets in water both below and above PNIPAAm's lower critical solution temperature (LCST), which implies a relatively high ratio of water molecules trapped in the nanostructures. As a result, largely reduced platelet adhesion is achieved on the as-prepared surface, both below and above LCST. It is demonstrated that the relatively high ratio of water molecules trapped in the nanostructures plays a key role in largely reducing the adhesion of platelets.

Conclusion and Outlook

This Account reviews recent progress on the design and synthesis of super-antiwetting interfaces with special adhesion, such as low adhesion, high adhesion, directional adhesion, and stimuli-responsive adhesion. Studies on the biological and bioinspired synthetic surfaces reveal that special designs of microstructures bring special adhesion properties. For instance, the topography and size of micro- and nanostructures have great influence on the value of liquid−solid adhesion, such as low and high adhesion. On the other hand, the arrangement and orientation of the micro- and nano structures may result in directional liquid−solid adhesion. Furthermore, reversible switching of adhesion between the low-adhesive rolling state and high-adhesive pinning state for a water droplet on a superhydrophobic surface could be achieved via cooperation of the stimuli-responsive materials and surface roughness. In addition, design of superoleophobic interfaces with special adhesion in an oil/water/solid system was also discussed. It was demonstrated that high content of water trapped in the micro- and nanostructures played a key role in reducing the adhesion of an oil droplet and platelets. These findings will bring a novel strategy to fabrication of antibioadhesion materials underwater.

The research on liquid−solid adhesion has just started, and numerous challenges remain in its development. First, the adhesion theories need to be further established. In fact, this closely associates with the development of experiment methods, especially on how to quantitatively study solid−liquid adhesive force along different directions. Second, the relation-

ship between the structure of biological surfaces and special adhesion needs to be further explored and revealed. Learning from nature will guide us to optimize the structure design of artificial surfaces. Finally, bioinspired materials should be "live" materials with various functions like organisms in nature. Therefore, *in situ* and rapid switching of adhesion will become one of our goals. In the future, we will further our research on the above aspects, with particular focus on bioinspired design of materials systems.

This work was supported by the grant of Major State Basic Research Development Program (2007CB936403), the National Nature Science Foundation of China (20571077).

BIOGRAPHICAL INFORMATION

Mingjie Liu received his B.S. degree in chemistry in Beijing University of Chemical and Technology (2005). In 2005, he joined Prof. Lei Jiang's group and received his M.S. degree in 2007. He is currently a Ph.D. student at National Center for Nanoscience and Technology, China (NCNST).

Yongmei Zheng obtained her Ph.D. from Jilin University of Technology in 2003. She worked as Postdoctoral fellow in Lei Jiang's group at the Institute of Chemistry, Chinese Academy of Sciences (ICCAS) (2003−2006) and then worked as scientific researcher at NCNST (2006−2008). She is currently associate professor at Beijing University of Aeronautics and Astronautics.

Jin Zhai received her Ph.D. from Peking University in Inorganic Chemistry in 1999. She worked as a postdoctoral fellow at ICCAS and then began an academic career there. Now, she is a professor at Beijing University of Aeronautics and Astronautics.

Lei Jiang received his B.S. degree (1987), M.S. degree (1990), and Ph.D. degree (1994) from Jilin University of China (Jintie Li's group). He then worked as a postdoctoral fellow in Prof. Akira Fujishima's group in Tokyo University. In 1996, he worked as a senior researcher in Kanagawa Academy of Sciences and Technology under Prof. Kazuhito Hashimoto. He joined ICCAS as part of the Hundred Talents Program in 1999. He is currently a professor at ICCAS.

FOOTNOTES

*To whom correspondence should be addressed. E-mail: jianglei@iccas.ac.cn.

REFERENCES

1 Feng, X. J.; Jiang, L. Design and creation of superwetting/antiwetting surfaces. *Adv. Mater.* **2006**, *18*, 3063–3078.

2 Feng, L.; Li, S. H.; Li, Y. S.; Li, H. J.; Zhang, L. J.; Zhai, J.; Song, Y. L.; Liu, B. Q.; Jiang, L.; Zhu, D. B. Super-hydrophobic surfaces: From natural to artificial. *Adv. Mater.* **2002**, *14*, 1857–1860.

3 Li, H. J.; Wang, X. B.; Song, Y. L.; Liu, Y. Q.; Li, Q. S.; Jiang, L.; Zhu, D. B. Super-"amphiphobic" aligned carbon nanotube films. *Angew. Chem., Int. Ed.* **2001**, *40*, 1743–1746.

4 Xi, J. M.; Feng, L.; Jiang, L. A general approach for fabrication of superhydrophobic and superamphiphobic surfaces. *Appl. Phys. Lett.* **2008**, *92*, 053102.

5 Liu, M. J.; Wang, S. T.; Wei, Z. X.; Song, Y. L.; Jiang, L. Bioinspired design of a superoleophobic and low adhesive water/solid interface. *Adv. Mater.* **2009**, *21*, 665–669.

6 Sun, T. L.; Feng, L.; Gao, X. F.; Jiang, L. Bioinspired surfaces with special wettability. *Acc. Chem. Res.* **2005**, *38*, 644–652.

7 Xia, F.; Jiang, L. Bio-inspired, smart, multiscale interfacial materials. *Adv. Mater.* **2008**, *20*, 2842–2858.

8 Blossey, R. Self-cleaning surfaces - virtual realities. *Nat. Mater.* **2003**, *2*, 301–306.

9 Cho, W. K.; Choi, I. S. Fabrication of hairy polymeric films inspired by geckos: Wetting and high adhesion properties. *Adv. Funct. Mater.* **2008**, *18*, 1089–1096.

10 Jin, M. H.; Feng, X. J.; Feng, L.; Sun, T. L.; Zhai, J.; Li, T. J.; Jiang, L. Superhydrophobic aligned polystyrene nanotube films with high adhesive force. *Adv. Mater.* **2005**, *17*, 1977–1981.

11 Winkleman, A.; Gotesman, G.; Yoffe, A.; Naaman, R. Immobilizing a drop of water: Fabricating highly hydrophobic surfaces that pin water droplets. *Nano Lett.* **2008**, *8*, 1241–1245.

12 Zhao, N.; Xie, Q. D.; Kuang, X.; Wang, S. Q.; Li, Y. F.; Lu, X. Y.; Tan, S. X.; Shen, J.; Zhang, X. L.; Zhang, Y.; Xu, J.; Han, C. C. A novel ultra-hydrophobic surface: Statically non-wetting but dynamically non-sliding. *Adv. Funct. Mater.* **2007**, *17*, 2739–2745.

13 Feng, L.; Zhang, Y. A.; Xi, J. M.; Zhu, Y.; Wang, N.; Xia, F.; Jiang, L. Petal effect: A superhydrophobic state with high adhesive force. *Langmuir* **2008**, *24*, 4114–4119.

14 Hong, X.; Gao, X. F.; Jiang, L. Application of superhydrophobic surface with high adhesive force in no lost transport of superparamagnetic microdroplet. *J. Am. Chem. Soc.* **2007**, *129*, 1478–1479.

15 Balu, B.; Breedveld, V.; Hess, D. W. Fabrication of "roll-off" and "sticky" superhydrophobic cellulose surfaces via plasma processing. *Langmuir* **2008**, *24*, 4785–4790.

16 Boduroglu, S.; Cetinkaya, M.; Dressick, W. J.; Singh, A.; Demirel, M. C. Controlling the wettability and adhesion of nanostructured poly-(p-xylylene) films. *Langmuir* **2007**, *23*, 11391–11395.

17 Huang, X. J.; Kim, D. H.; Im, M.; Lee, J. H.; Yoon, J. B.; Choi, Y. K. Lock-and-key" geometry effect of patterned surfaces: Wettability and switching of adhesive force. *Small* **2009**, *5*, 90–94.

18 Lai, Y. K.; Lin, C. J.; Huang, J. Y.; Zhuang, H. F.; Sun, L.; Nguyen, T. Markedly controllable adhesion of superhydrophobic spongelike nanostructure TiO_2 films. *Langmuir* **2008**, *24*, 3867–3873.

19 Song, X. Y.; Zhai, J.; Wang, Y. L.; Jiang, L. Fabrication of superhydrophobic surfaces by self-assembly and their water-adhesion properties. *J. Phys. Chem. B* **2005**, *109*, 4048–4052.

20 Zhao, Y.; Lu, Q. H.; Chen, D. S.; Wei, Y. Superhydrophobic modification of polyimide films based on gold-coated porous silver nanostructures and self-assembled monolayers. *J. Mater. Chem.* **2006**, *16*, 4504–4509.

21 Cheng, Z. J.; Feng, L.; Jiang, L. Tunable adhesive superhydrophobic surfaces for superparamagnetic microdroplets. *Adv. Funct. Mater.* **2008**, *18*, 3219–3225.

22 Li, C.; Guo, R. W.; Jiang, X.; HU, S. X.; Li, L.; Cao, X. Y.; Yang, H.; Song, Y. L.; Ma, Y. M.; Jiang, L. Reversible switch of water droplet mobility on superhydrophobic surface based on phase transition of SCLPC *Adv. Mater.* **2009**, *21*, 4254 −4258.

23 Lafuma, A.; Quéré, D. Superhydrophobic states. *Nat. Mater.* **2003**, *2*, 457–460.

24 Quéré, D.; Lafuma, A.; Bico, J. Slippy and sticky microtextured solids. *Nanotechnology* **2003**, *14*, 1109–1112.

25 Patankar, N. A. Transition between superhydrophobic states on rough surfaces. *Langmuir* **2004**, *20*, 7097–7102.

26 Chen, W.; Fadeev, A. Y.; Hsieh, M. C.; Öner, D.; Youngblood, J.; McCarthy, T. J. Ultrahydrophobic and ultralyophobic surfaces: Some comments and examples. *Langmuir* **1999**, *15*, 3395–3399.

27 Yoshimitsu, Z.; Nakajima, A.; Watanabe, T.; Hashimoto, K. Effects of surface structure on the hydrophobicity and sliding behavior of water droplets. *Langmuir* **2002**, *18*, 5818–5822.

28 Wenzel, R. N. Resistance of solid surfaces to wetting by water. *Ind. Eng. Chem.* **1936**, *28*, 988–994.

29 Cassie, A. B. D.; Baxter, S. Wettability of porous surfaces. *Trans. Faraday Soc.* **1944**, *40*, 0546−0550.

30 Marmur, A. The lotus effect: Superhydrophobicity and metastability. *Langmuir* **2004**, *20*, 3517–3519.

31 Barbieri, L.; Wagner, E.; Hoffmann, P. Water wetting transition parameters of perfluorinated substrates with periodically distributed flat-top microscale obstacles. *Langmuir* **2007**, *23*, 1723–1734.

32 Extrand, C. W. Criteria for ultralyophobic surfaces. *Langmuir* **2004**, *20*, 5013–5018.

33 He, B.; Patankar, N. A.; Lee, J. Multiple equilibrium droplet shapes and design criterion for rough hydrophobic surfaces. *Langmuir* **2003**, *19*, 4999–5003.

34 Joanny, J. F.; Degennes, P. G. A Model for contact-angle hysteresis. *J. Chem. Phys.* **1984**, *81*, 552–562.

35 Johnson, R. E.; Dettre, R. H. Contact angle hysteresis. III. Study of an idealized heterogeneous surface. *J. Phys. Chem.* **1964**, *68*, 1744–1750.

36 Kusumaatmaja, H.; Yeomans, J. M. Modeling contact angle hysteresis on chemically patterned and superhydrophobic surfaces. *Langmuir* **2007**, *23*, 6019–6032.

37 McHale, G.; Shirtcliffe, N. J.; Newton, M. I. Contact-angle hysteresis on super-hydrophobic surfaces. *Langmuir* **2004**, *20*, 10146–10149.

38 Zhang, J. F.; Kwok, D. Y. Contact line and contact angle dynamics in superhydrophobic channels. *Langmuir* **2006**, *22*, 4998–5004.

39 Nosonovsky, M. Model for solid-liquid and solid-solid friction of rough surfaces with adhesion hysteresis. *J. Chem. Phys.* **2007**, *126*, 224701.

40 Wang, S.; Jiang, L. Definition of superhydrophobic states. *Adv. Mater.* **2007**, *19*, 3423–3424.

41 Gao, X. F.; Jiang, L. Water-repellent legs of water striders. *Nature* **2004**, *432*, 36.

42 Zheng, Y. M.; Han, D.; Zhai, J.; Jiang, L. In situ investigation on dynamic suspending of microdroplet on lotus leaf and gradient of wettable micro- and nanostructure from water condensation. *Appl. Phys. Lett.* **2008**, *92*, 084106.

43 Chen, P. P.; Chen, L.; Han, D.; Zhai, J.; Zheng, Y. M.; Jiang, L. Wetting behavior at micro-/nanoscales: Direct imaging of a microscopic water/air/solid three-phase interface. *Small* **2009**, *5*, 908–912.

44 Zhang, J. H.; Wang, J. M.; Zhao, Y.; Xu, L.; Gao, X. F.; Zheng, Y. M.; Jiang, L. How does the leaf margin make the lotus surface dry as the lotus leaf floats on water. *Soft Matter* **2008**, *4*, 2232–2237.

45 Autumn, K.; Liang, Y. A.; Hsieh, S. T.; Zesch, W.; Chan, W. P.; Kenny, T. W.; Fearing, R.; Full, R. J. Adhesive force of a single gecko foot-hair. *Nature* **2000**, *405*, 681–685.

46 Lai, Y. K.; Gao, X. F.; Zhuang, H. F.; Lin, C. J.; jiang, L. Designing superhydrophobic porous nanostructures with tunable water adhesion. *Adv. Mater.* **2009**, *21*, 3799–3803.

47 Xi, J.; Jiang, L. Biomimic superhydrophobic surface with high adhesive forces. *Ind. Eng. Chem. Res.* **2008**, *47*, 6354–6357.

48 Daniel, S.; Chaudhury, M. K.; de Gennes, P. G. Vibration-actuated drop motion on surfaces for batch microfluidic processes. *Langmuir* **2005**, *21*, 4240–4248.

49 Extrand, C. W. Retention forces of a liquid slug in a rough capillary tube with symmetric or asymmetric features. *Langmuir* **2007**, *23*, 1867–1871.

50 Zheng, Y. M.; Gao, X. F.; Jiang, L. Directional adhesion of superhydrophobic butterfly wings. *Soft Matter* **2007**, *3*, 178–182.

51 Zhang, J. H.; Cheng, Z. J.; Zheng, Y. M.; Jiang, L. Ratchet-induced anisotropic behavior of superparamagnetic microdroplet. *Appl. Phys. Lett.* **2009**, *94*, 144104.

52 Nosonovsky, M.; Bhushan, B. Biomimetic superhydrophobic surfaces: Multiscale approach. *Nano Lett.* **2007**, *7*, 2633–2637.

53 Krupenkin, T. N.; Taylor, J. A.; Schneider, T. M.; Yang, S. From rolling ball to complete wetting: The dynamic tuning of liquids on nanostructured surfaces. *Langmuir* **2004**, *20*, 3824–3827.

54 Tian, D. L.; Chen, Q. W.; Nie, F. Q.; Xu, J. J.; Song, Y. L.; Jiang, L. Patterned wettability transition by photoelectric cooperative and anisotropic wetting for liquid reprography. *Adv. Mater.* **2009**, *21*, 3744–3749.

55 Chen, L.; Liu, M. J.; Bai, H.; Chen, P. P.; Xia, F.; Han, D.; Jiang, L. Antiplatelet and thermally responsive poly(*N*-isopropylacrylamide) surface with nanosclae topography. *J. Am. Chem. Soc.* **2009**, *131*, 10467–10472.